High-harmonic generation by quantum-dot nanorings

Ioan Bâldea,[1,*] Ashish K. Gupta,[2,†] Lorenz S. Cederbaum,[1] and Nimrod Moiseyev[2]
[1]*Theoretische Chemie, Physikalisch-Chemisches Institut, Universität Heidelberg, Im Neuenheimer Feld 229, D-69120 Heidelberg, Germany*
[2]*Department of Chemistry and Minerva Center of Nonlinear Physics in Complex Systems Technion-Israel Institute of Technology, Haifa 32000, Israel*
(Received 30 January 2004; published 18 June 2004)

Exact numerical results are obtained within the extended Hubbard Hamiltonian for nanorings consisting of Ag quantum dots (QD's) with C_{6v} symmetry which interact with a circularly polarized light. The results show that the high-harmonic generation (HHG) spectra obtained from such artificial "molecules" are more pronounced than the HHG spectra obtained from a real molecule such as benzene. Our studies show that the HHG spectra obtained from the QD nanorings consist of two plateaus while only one plateau appears for benzene. The role of electron correlations in the generation of the high-order harmonics is studied, and it is shown that it can increase the intensity of the high-order harmonics. Mainly affected are the harmonics which are located in the second plateau. Selection rules for the produced high harmonics and a new "synergetic" selection rule for the symmetry of the states contributing to the HHG spectrum, a combined effect of spatial and charge conjugation symmetries, are discussed.

DOI: 10.1103/PhysRevB.69.245311 PACS number(s): 78.67.−n, 42.65.Ky, 68.65.Hb, 73.63.−b

I. INTRODUCTION

The phenomenon of high harmonic generation (HHG) in atomic gases has been extensively studied both experimentally and theoretically in the past twenty years (see, e.g., Ref. 1, and references therein) and in molecular gases since the mid-1990's.[2–5] A common characteristic of HHG-based radiation sources is their multichromaticity. The fact that the HHG spectra obtained for atomic gases consists only of odd-order high harmonics up to a certain cutoff has been explained by combining the *spherical* symmetry of atoms and the monochromaticity of the linearly polarized laser field (see, e.g., Ref. 6). However, this explanation is based on perturbation theory, and thus breaks down and does not hold for the high intensity lasers which are applied in order to generate the high-order harmonics. A nonperturbative proof has been given under the assumption that the photoinduced dynamics is controlled by a *single* resonance quasienergy Floquet state taking into consideration in the analysis of the dynamical symmetry the symmetry of the system which interacts with the electromagnetic laser field.[7,8] The dynamical symmetry analysis indicated that the difference between atomic and molecular HHG is probably most striking in the case of interaction with a circular polarized laser field. For symmetry reasons, atoms interacting with a circular polarized field do not generate harmonics of the incident radiation frequency. However, the interaction of aligned molecules (and also thin crystal[8] and nanotubes)[9] possessing N th-order rotational symmetry with a circular polarized field brings about HHG with unusual selection rules: the emitted high-order harmonic frequencies are $\Omega=\omega,(lN\pm1)\omega$, $l=1,2,\ldots$,where ω is the fundamental frequency. The $(lN+1)$th harmonics are polarized circularly as the incident field, while the $(lN-1)$th harmonics are polarized circularly in the opposite way.

Recent theoretical studies carried out by Žďánská and her co-workers[10] for model benzene molecule at the laser wavelength of 800 nm have shown that the emitted harmonics possess the frequencies $(6\pm1)\omega,(12\pm1)\omega,\ldots$, also when the laser polarization deviates from the "ideal" circular one by about 5%. Another important result is that the nonlinear response of the model benzene molecule is found to originate mainly from the field-induced transitions between the bound states, in accordance with the earlier analytical theory.[11] The fact that when a circularly laser field is applied, the HHG spectra is obtained from bound-to-bound state transitions (of the field-free molecule) and *not* from bound-continuum transitions implies that the high-order harmonics are *not* generated due to the semiclassical mechanism. In this mechanism, the electron is released to the continuum with nearly zero velocity, either via tunneling or multiphoton process, accelerated by the field, and eventually revisits the ionic core and recombines while emitting high energy photons (harmonics). In our case, where a molecule or a QD ring with $C_{N,v}$ symmetry interacts with circularly polarized light, the high-order harmonics are generated by electronic excitations. The one-electron effective potential calculations carried out for benzene,[8] the 2D one-electron calculations for benzene where ionization was considered,[10] and the treatment of the problem on the density functional theory level,[12] all show that the generation of high-order harmonics when circularly polarized laser is applied proceeds via bound-to-bound state transitions.

The main purpose of this paper is to study the HHG spectra for nanorings with C_{6v} symmetry consisting of Ag QD's which interact with a circularly polarized light. In the absence of the electron-nuclei attraction potential terms, the mechanism for generating high-order harmonics is expected to be very different from that in atoms and molecules. Individual QD's behave as artificial atoms;[13] being confined within a few nanometers, electrons occupy quantized levels analogous to atomic orbitals in ordinary atoms. Most electrons are localized on individual QD's. However, a small

 ©2004 The American Physical Society

number of ("valence") electrons are bound weakly enough to become delocalized over the whole "artificial" molecule if the overlap of their wave functions for adjacent QD's is large enough. The salient feature of such artificial atoms and molecules is that, unlike the natural counterparts, their electronic properties can be *tuned* continuously by varying the dot diameter $2R$ and/or interdot spacing D.

In view of their tunable properties, assemblies of QD's represent ideal controllable systems for studying many aspects unexplored so far for strongly correlated electrons. The numerical results presented here indicate that, already with achievements of present nanotechnologies,[14] (i) "artificial" molecules (circular arrays of nanorings of QD's) appear to be more promising for higher harmonic generation than ordinary molecules and (ii) electron correlation effects play an important role in such nanorings.

The remaining part of this paper is organized as follows. In Sec. II we introduce the model of nanorings and describe the method of solution. Results on HHG spectra both for QD nanorings and for the benzene molecule are presented in Sec. III. Effects of electron correlations on the HHG spectra are discussed in Sec. IV in connection to scaling properties of the investigated model. Some discussions and conclusions make the object of the final Sec. V.

II. MODEL AND METHOD

In the present paper, we consider nanorings consisting of $N=6$ QD's. To describe the delocalized ("valence" or "π") electrons in a nanoring we shall use an extended Hubbard (in chemists' nomenclature, Pariser-Parr-Pople) model Hamiltonian H

$$H = -\beta_0 \sum_{l=1}^{N} \sum_{\sigma=\uparrow,\downarrow} (a_{l,\sigma}^{\dagger} a_{l+1,\sigma} + a_{l+1,\sigma}^{\dagger} a_{l,\sigma}) + \sum_{l=1}^{N} (U\mathcal{N}_{l,\uparrow}\mathcal{N}_{l,\downarrow} + V\mathcal{N}_l\mathcal{N}_{l+1}), \quad (1)$$

where, $a(a^{\dagger})$ denote creation (annihilation) operators for valence electrons, $\mathcal{N}_{l,\sigma} \equiv a_{l,\sigma}^{\dagger} a_{l,\sigma}$, $\mathcal{N}_l \equiv \mathcal{N}_{l,\uparrow} + \mathcal{N}_{l,\downarrow}$. Each QD is modeled by a single "atomic" orbital. Individual QD's are characterized by the on-site Coulomb repulsion energy U (related to self-elastance, or Coulomb blockade) and the energy of valence electrons ϵ, set zero in Eq. (1). QD's are coupled by electron tunneling (resonance integral β_0) and Coulomb interaction V (related to the mutual elastance). Basically, U and ϵ depend on R, whereas β_0 and V depend on D.

There are several reasons for choosing six-site nanorings described by the model Hamiltonian of Eq. (1). An important aim of the present study is to compare harmonic generation spectra of "artificial" molecules and ordinary cyclic molecules. Obviously, such a comparison is most relevant when both kinds of systems can be described by similar models. We have chosen presumably the most common example of the latter class, the benzene molecule ($N=6$); it belongs to the class of cyclic polyenes, just the kind of molecules for which the Pariser-Parr-Pople model was initially proposed (see, e.g., Ref. 15). In principle, model calculations based on Eq. (1) can be performed for a ring containing $N_{\mathrm{el}} = 1, \ldots, 2N-1$ delocalized (π) electrons. However, since the benzene molecule contains six π electrons and six CH units, a nanoring at half-filling ($N_{\mathrm{el}}=N=6$) appears most interesting. In fact, previous theoretical studies[16–19] have also considered the model Hamiltonian of Eq. (1) in the half-filling case and were able to successfully reproduce a variety of experimental data in assembled QD's of silver.[14] In the present paper, we shall also focus our attention to the same type of QD's.

Let us briefly describe the method to determine the parameters for Ag QD's with $2R=2.6$ nm.[16,19] The interdot separation $d \equiv D/(2R)$ (measured between QD centers) has been continuously varied in the range $1.10 \lesssim d \lesssim 1.85$, allowing a wide tuning of various physical properties.[14] This is mainly due to the exponential behavior found for $\beta_0[\propto \exp(-5.5d)]$,[17] analogous to polyenes.[20] For $d=1.2$, a value $\beta_0=0.5$ eV has been extracted by fitting experimental data.[16] For Ag QD's with $2R=2.6$ nm examined here, Coulomb blockade experiments, using scanning tunneling microscopy (STM), led to $U=0.34$ eV, in agreement with the estimate $U=e^2/(\varepsilon R)$ deduced by assuming a spheric Ag core in a medium of dielectric constant $\varepsilon \simeq 2-3$.[14,21]

Intuitively, one expects an intersite Coulomb repulsion V weaker than the on-site repulsion U. To estimate V and U we have used the same method developed by two of us,[19] computing the mutual- and self-elastances, respectively deduced numerically by using formulas of classical electrostatics[22] for two identical spheres. Let us note also note that in Eq. (1) we have assumed an ideal situation, where the model parameters are site independent.[23] This can be considered a reasonable first-order approximation in view of the narrow size distributions ($\sim 5\%$) in the arrays of Ag QD's assembled by Heath's group.[14]

To determine the model parameters for benzene, one can fix β_0 to its "spectroscopic" value ($\beta_0=2.5$ eV) and adjust U and V to fit eight quantities, namely the experimental excitation energies $^3B_{1u}$, $^3E_{1u}$, $^1B_{2u}$, $^3B_{2u}$, $^1B_{1u}$, $^3B_{2g}$, $^1E_{1u}$, and $^1E_{2g}$ (D_{6h} notation).[24] By choosing $U=4.5$ eV and $V=1.3$ eV one can reproduce remarkably well *all* the aforementioned energies;[25] the highest error does not exceed 0.5 eV. Noteworthy, this accuracy is comparable to that of *ab initio* quantum chemical computations superseding nowadays the semiempirical Pariser-Parr-Pople model.

Below, we shall present results on the harmonic generation spectrum of a six-site nanoring placed in a strong laser field H_{field} assumed to be circularly polarized. So, the dynamics of the system is governed by the total time-dependent Hamiltonian $H_T(t)$

$$H_T(t) = H + H_{\mathrm{field}}(t) = H - \mathbf{P} \cdot \mathbf{E}(t), \quad (2)$$

where $\mathbf{P}$ is the electric dipole operator

$$\mathbf{P} = -|e|\rho \sum_l \mathcal{N}_l \left[\hat{\mathbf{x}} \cos\frac{2\pi l}{N} + \hat{\mathbf{y}} \sin\frac{2\pi l}{N} \right]. \quad (3)$$

Here, e denotes the elementary charge and ρ stands for the ring radius ($\rho=D$ for $N=6$). For a circularly polarized laser

radiation, the electric field reads $\mathbf{E}(t)=E_0(\hat{\mathbf{x}}\cos\omega t+\hat{\mathbf{y}}\sin\omega t)$.

In our current study we ignore losses due to ionization of the array of quantum dots. In atoms, for instance, it is known that ionization starts to be relevant from intensities of 10^{14} W/cm^2 on.[26] The relevant intensities for quantum dots are not known, but we assume that even at the highest intensities we use here (close to 10^{13} W/cm^2) the losses due to ionization are not crucial.

To compute the exact harmonic generation spectra, the knowledge of the eigenstates Ψ_j of H, Eq. (1), is necessary to calculate the matrix elements of the dipole operator $\mathbf{P}$. However, the time propagation is very time consuming when using all eigenstates Ψ_j (see the discussion at the end of this section). Significant gain can be obtained by exploiting the spatial symmetry [point group D_{6h} (Ref. 24)] and the fact that both the total spin and total spin projection are good quantum numbers. In this paper we shall assume that the initial state of the the ring is its ground state Ψ_G, which is a singlet of symmetry A_{1g}. Because the dipole operator $\mathbf{P}$ does not change the total spin, only eigenstates which are singlets are needed for propagation. This results in a reduction of the dimension of the Hilbert space from 924 to 175.[27] The spatial symmetry of these 175 singlet states is as follows: 22 A_{1g} states, 10 A_{2g} states, 16 B_{1u} states, 13 B_{2u} states, 60 E_{2g} states, and 54 E_{1u} states. One can easily show that the dipole operator $\mathbf{P}$ possesses E_{1u} symmetry, and therefore only eigenstates Ψ_j and Ψ_k whose product transforms according to an E_{1u} irreducible representation yields nonvanishing dipole matrix elements. In view of the multiplication table of the group D_{6h}, couplings via dipole transition are possible only between two eigenstates according to the following:

$$A_{1g}\times E_{1u}=E_{1u},$$

$$A_{2g}\times E_{1u}=E_{1u},$$

$$B_{1u}\times E_{2g}=E_{1u},$$

$$B_{2u}\times E_{2g}=E_{1u},$$

$$E_{2g}\times E_{1u}=B_{1u}+B_{2u}+E_{1u}. \tag{4}$$

Consequently, the coupling scheme

$$\begin{array}{c} A_{1g}\leftrightarrow E_{1u}\leftrightarrow A_{2g} \\ \updownarrow \\ B_{1u}\leftrightarrow E_{2g}\leftrightarrow B_{2g} \end{array} \tag{5}$$

holds for the transitions within our system coupled by the dipole operator.

One should note that Eqs. (4) and (5) indicate dipole transitions allowed by the *spatial* symmetry D_{6h} alone. Fortunately, a further reduction of the total number of eigenstates which contribute to the HHG spectra is possible. This is due to a special property of the model Hamiltonian of Eq. (1) in the half-filling case considered in the present paper, namely, the charge conjugation (also termed particle-hole) symmetry; see, e.g., Refs. 28, and references cited therein. The eigenstates of H are either even or odd with respect to the charge conjugation transformation[28]

$$a_{l,\sigma}\rightarrow a^{\dagger}_{l,\sigma} \quad \text{and} \quad a^{\dagger}_{l,\sigma}\rightarrow a_{l,\sigma}. \tag{6}$$

We shall denote this by an extra superscript "+" or "−," respectively. With the aid of this index for charge conjugation one can further specify the eigenstates; there are 18 A^{+}_{1g}, 4 A^{-}_{1g}, 2 A^{+}_{2g}, 8 A^{-}_{2g}, 3 B^{+}_{1u}, 13 B^{-}_{1u}, 9 B^{+}_{2g}, 4 B^{-}_{2g}, 22 E^{+}_{1u}, 32 E^{-}_{1u}, 36 E^{+}_{2g}, and 24 E^{-}_{2g} eigenstates. As one can easily demonstrate if one makes use of Eq. (3) for $\mathbf{P}$ given above, the dipole operator is odd ($\mathbf{P}\rightarrow-\mathbf{P}$) with respect to the charge conjugation, Eq. (6). Consequently, dipole transitions are allowed only between eigenstates of *opposite* parities. In view of these considerations, the coupling scheme (5) can be further detailed and breaks down into two independent schemes

$$\begin{array}{c} (18)A^{+}_{1g}\leftrightarrow(32)E^{-}_{1u}\leftrightarrow(2)A^{+}_{2g} \\ \updownarrow \\ (13)B^{-}_{1u}\leftrightarrow(36)E^{+}_{2g}\leftrightarrow(4)B^{-}_{2g} \end{array} \tag{7}$$

and

$$\begin{array}{c} (4)A^{-}_{1g}\leftrightarrow(22)E^{+}_{1u}\leftrightarrow(8)A^{-}_{2g} \\ \updownarrow \\ (3)B^{+}_{1u}\leftrightarrow(24)E^{-}_{2g}\leftrightarrow(9)B^{+}_{2g}. \end{array} \tag{8}$$

Above, the entries in parentheses specify the numbers of eigenstates with a certain symmetry. A straightforward analysis based on Eqs. (7) and (8) reveals that there exist two blocks containing 105 and 70 eigenstates, respectively which do not interact to each other via dipole transitions. By noting furthermore that the ground state is an A^{+}_{1g} state, one can conclude that, out of a total number of 924 eigenstates, only 105 eigenstates [namely, those entering Eq. (7)] contribute to the harmonic generation spectrum of a six-QD nanoring in the ground state. These 105 eigenstates are coupled among themselves according to Eq. (7). A further interesting point revealed by our numerical calculations is that the states of either block whose couplings are allowed by symmetry *do* couple indeed; so, there are *no* other transitions forbidden, e.g., dynamically.

To perform time propagation, we have employed the (t,t') method. A comprehensive description of this method can be found in the reviews of Refs. 29. Here, we restrict ourselves to present a few relevant details. By using the (t,t') method, one can get the solution of the time-dependent Schrödinger equation $|\Psi(t)\rangle$ avoiding the complication arising from the fact that the Hamiltonian is time dependent and one has to consider time-ordering operators.[30] The (t,t') method enables us to express the time evolution operator as $\hat{U}(t\leftarrow t')=\exp[-i\mathcal{H}_T(t')t]$, where $\mathcal{H}_T(t')=-i\,\partial/\partial t'+H_T(t')$. The time-dependent wave function is given by $\Psi(t)=[\hat{U}(t\leftarrow t')\Psi(t=0)]_{t'=t}$, where $\Psi(0)$ is the ground eigenstate of the field-free Hamiltonian H as defined in Eq. (1). $\Psi(t)$ can be expanded as a linear combination of the quasienergy Floquet states $\Phi_{\epsilon}(t)$

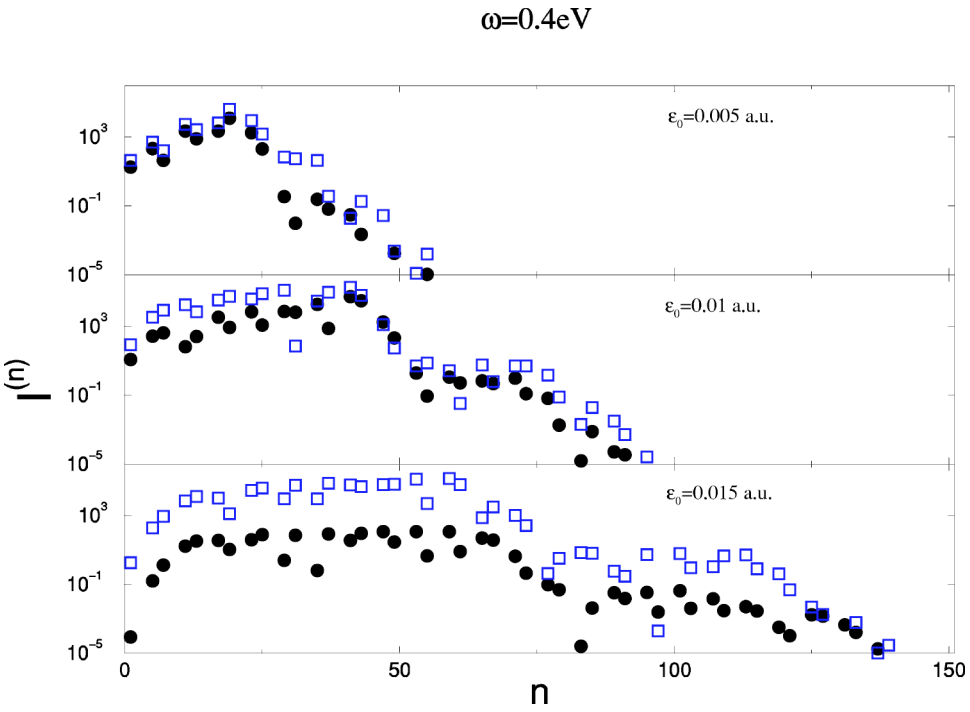

FIG. 1. High harmonic generation spectra for nanorings consisting of six Ag quantum dots (intradot separation $d=1.3$) interacting with a circularly polarized light. Full circles are exact results, open squares correspond to a single Floquet state approximation (see the main text).

$$|\Psi(t)\rangle = \sum_{\epsilon} a_{\epsilon} \exp(-i\epsilon t)|\Phi_{\epsilon}(t)\rangle, \tag{9}$$

where $\Phi_{\epsilon}(t)=\Phi_{\epsilon}(t+T)$ are the time-periodic $(T\equiv 2\pi/\omega)$ eigenfunctions of the Floquet Hamiltonian $\mathcal{H}_T(t)|\Phi_{\epsilon}(t)\rangle = \epsilon|\Phi_{\epsilon}(t)\rangle$. The expansion coefficients a_{ϵ} are determined by specifying the initial state, taken here to be the ground state of the field-free system

$$|\Psi_G\rangle = |\Psi(t=0)\rangle = \sum_{\epsilon} a_{\epsilon}|\Phi_{\epsilon}(t=0)\rangle. \tag{10}$$

The HHG spectrum is associated with the nth components of the time Fourier transform of the two quantities

$$\frac{\partial^2}{\partial t^2}\langle\Psi(t)|P_{\pm}|\Psi(t)\rangle \propto \frac{\partial^2}{\partial t^2}\left\langle \Psi(t)\left|\sum_l \mathcal{N}_l \exp\left(\pm\frac{2\pi l}{N}i\right)\right|\Psi(t)\right\rangle.$$

Here, $P_{\pm}\equiv P_x \pm iP_y$, the cartesian components of the dipole operator **P** being expressed by Eq. (3), and the subscript $+(-)$ refers to harmonics of orders $n=6m+1$ $(n=6m-1)$ which are circularly polarized as (opposite to) the circularly polarized incident radiation. Their intensities $I_{\pm}^{(n)}$ can be expressed as

$$I_{\pm}^{(n)} \propto n^4 \left|\sum_{\epsilon}\int_0^T dt|a_{\epsilon}|^2\exp(-in\omega t)\langle\Phi_{\epsilon}(t)|P_{\pm}|\Phi_{\epsilon}(t)\rangle\right|^2. \tag{11}$$

One should note that, according to Eq. (11), there is no interference between the contributions of the different Floquet states $\Phi_{\epsilon}(t)$.

A virtue of the (t,t') method is that it allows us to use a small number of Floquet channels N_c (typically, $N_c=7$), even when the field intensity is very large. For rings with six sites and six electrons, the dimension of the Hilbert space is $D=924$, and the corresponding 924 eigenstates can and have been computed without difficulty by means of exact numerical diagonalization. Nevertheless, by using all these 924 eigenstates, the time propagation is very time consuming. For example, even when a small number of Floquet channels is taken into account in the numerical calculations, the construction of the time evolution operator $\hat{U}[m\tau\leftarrow(m-1)\tau]$, where τ is a small time step, requires about

$$(DN_c)^3 \simeq \begin{cases} 3\times 10^{11} & \text{for } D=924, N_c=7, \\ 4\times 10^{8} & \text{for } D=105, N_c=7 \end{cases} \tag{12}$$

numerical operations. However, in order to construct $U(t\leftarrow 0)$ one should calculate the product $\Pi_{m=1}^{M}U[m\tau\leftarrow(m-1)\tau]$, where $M=T/\tau$ and $T=2\pi/\omega$. This analysis explains why the computation time for propagation is very large even when an efficient method as the (t,t') method has been used, and why a reduction in the number of eigenstates used in the numerical calculations is most desirable.

III. RESULTS FOR HHG SPECTRA

Our computed results on the HHG production are collected in the spectra depicted in Figs. 1 and 2. The full circles shown represent the results obtained from the full calculations. In these calculations the contributions of all the Floquet states have been included. For the sake of comparison, we have also computed the HHG spectra assuming that the photoinduced dynamics is controlled by a single quasienergy Floquet eigenstate $\Phi_{\mathrm{QE}}(t)$. This state $\Phi_{\mathrm{QE}}(t)$ has been chosen as the Floquet state $\Phi_{\epsilon_{\max}}(t)$ of quasienergy $E_{\mathrm{QE}}=\epsilon_{\max}$ which

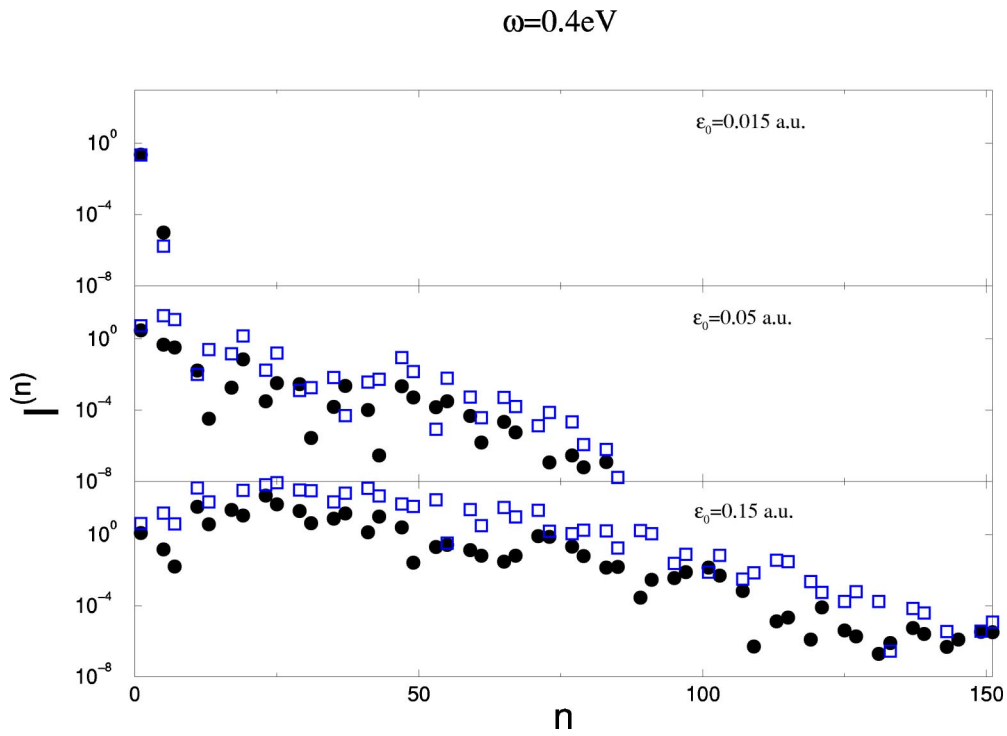

FIG. 2. High harmonic generation spectra for a benzene molecule modeled by Hamiltonian (1). The symbols have the same meaning as in Fig. 1.

has the largest overlap with the field-free ground state Ψ_G, $|a_{\epsilon_{\max}}| \equiv \max_\epsilon |a_\epsilon| = \max_\epsilon |\langle \Phi_\epsilon(t=0) | \Psi_G \rangle|$ [see Eq. (10)]. With a single state, the wave function $\Psi(t)$ takes on the appearance $\Psi(t) = \exp(-iE_{\mathrm{QE}}t)\Phi_{\mathrm{QE}}(t)$. The corresponding single-state HHG spectra are shown as open squares in Figs. 1 and 2.

Although the individual intensities of the high harmonics are not quantitatively reproduced by this single-state approximation, the latter does reproduce the overall appearance of the exactly computed spectra, for instance, the plateaus. This is very interesting, since in high intensity fields the initial field-free state populates many Floquet states.[31]

In Figs. 1 and 2, the HHG spectra are presented for the circular QD array (interdot distance $d=1.3$) and for benzene model Hamiltonian, respectively, when the laser frequency is held fixed (photon energy $\hbar\omega=0.4$ eV) and the maximum field amplitude ϵ_0 is varied. The laser intensity is given by I_0 (W/cm^2) $= 2 \times 3.5 \times 10^{16} \epsilon_0^2$ (a.u.), where the factor 2 is due to the use of circularly polarized light. For example, when $\epsilon_0 = 0.015$ a.u. and the field intensity is equal to 7.9×10^{12} W/cm^2, an extended plateau in the HHG spectra is obtained for the QD nanorings, whereas, practically, no high-order harmonics are obtained from benzene at the same laser intensity. As one can see for the QD nanorings, high-order harmonics are obtained for fields which are much weaker than the fields which have to be used for benzene.

In both cases (i.e., QD's and benzene molecule) the HHG spectra satisfy the selection rules mentioned in Sec. I: the emitted high-order harmonics are $6\pm1, 12\pm1, 18\pm1, \ldots, 6m\pm1, \ldots$. Another interesting result is that the HHG spectra obtained from QD arrays (see Fig. 1) consist of two plateaus (actually even more, but only two are quantitative significant). Such phenomena have been also reported for atoms when the relative phase between two color lasers has been varied.[32] These phenomena can be explained classically. The interpretation to our case is that the extended plateau (i.e., two or more plateaus) results from the different possible trajectories of the electrons which reach one of the sites (QD's or CH units in the simple model of benzene) with a maximal velocity. If, for example, the high-order harmonics results from the revisit of the electrons at their original site, only one plateau might be obtained. The study of a classical mechanism of this kind is, however, beyond the scope of the present work.

IV. SCALING AND ELECTRON CORRELATION EFFECTS ON HHG

In the case $U=V=0$, Eq. (1) describes a periodic system of free electrons characterized by wave functions of plane wave type. Then, one can easily see from Eqs. (1) and (2) that the time-dependent Schrödinger equation of Hamiltonian $H_T(t)$ leads to a harmonic generation spectrum independent on the interdot distance d if the field strength and the laser frequency are scaled according to the following transformation:

$$\epsilon_0(d) = \epsilon_{0,\mathrm{ref}} \xi(d)/\eta(d), \quad \omega(d) = \omega_{\mathrm{ref}} \xi(d), \tag{13}$$

where d_{ref}, $\epsilon_{0,\mathrm{ref}}$, and ω_{ref} are reference parameters, and the scaling parameters ξ and η are defined by

$$\xi(d) = \beta_0(d)/\beta_0(d_{\mathrm{ref}}), \quad \eta(d) = d/d_{\mathrm{ref}}. \tag{14}$$

This invariance of the spectrum is exact; it can be proven mathematically for the free electron system ($U=V=0$). Be-

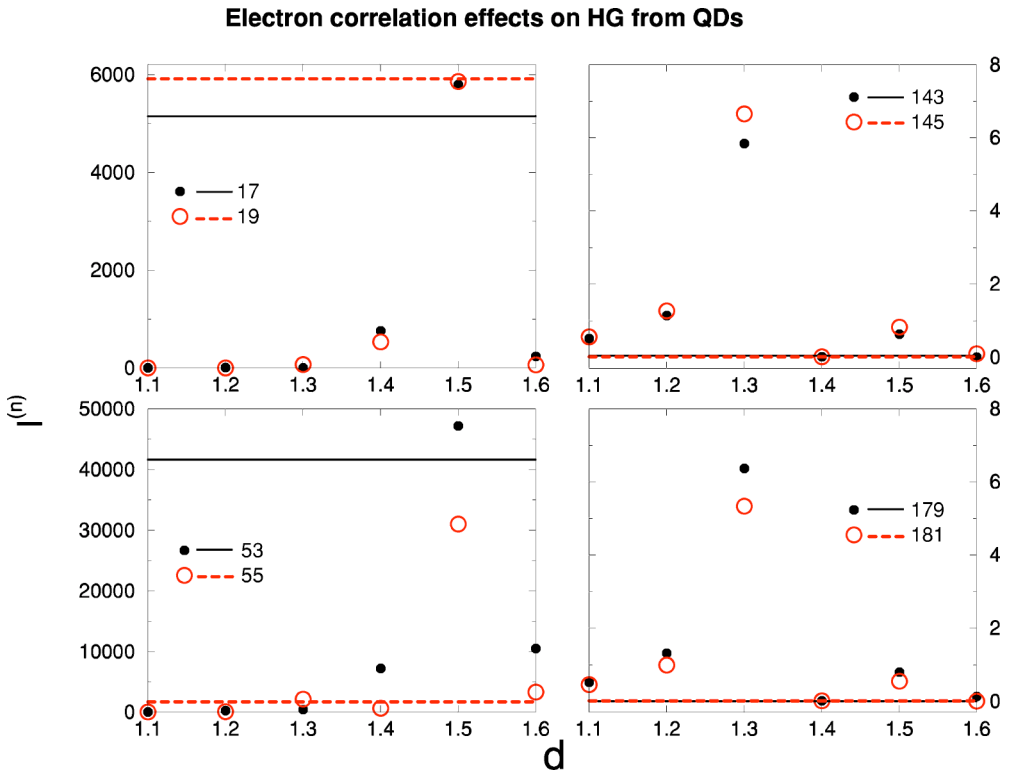

FIG. 3. The impact of correlation effects on high-order harmonics belonging to the first plateau [the pairs of (17, 19) and (53, 55) harmonics] and to the second plateau [the pairs of (143, 145) and (179, 181) harmonics] of the HHG spectra as a function of the interdot separation d. Neglecting electron correlations, the intensity $I^{(n)}$ does not depend on d and is represented by a horizontal line. For each harmonic, the deviation of the points (full calculations, i.e., including electron correlations) from the corresponding horizontal line (results without correlations) is a measure of the strength of electron correlations. In each panel, a given harmonic has its own horizontal line (solid or dashed) and point style (filled or opened circles, respectively), both specified in inset.

cause the plane waves also satisfy the Hartree-Fock equations,[33] one can relate the aforementioned invariance to the lack of electron correlations. One can check straightforwardly that this invariance does not hold anymore for the correlated electron system described by the Hamiltonian of Eq. (1) with $U, V \neq 0$. We have exploited this scaling to evidence electron correlation effects. Namely, we have performed exact calculations for various d values with the parameters scaled according to Eqs. (13) and (14), and inspected the d dependence of the intensity of the various harmonics $I^{(n)}$; the magnitude of the deviation from a horizontal straight line is a direct measure of electron correlations.

In the calculations reported here we have chosen a reference value $d_{\mathrm{ref}}=1.1$, i.e., corresponding to QD's sufficiently close to each other, for which the electronic bandwidth $4\beta_0$ is sufficiently larger than U and V, and electron correlations are weak (see, e.g., Ref. 19). The reference laser frequency ω_{ref} has been chosen to be resonant with the highest intensity dipole transition from the ground state. Finally, the reference field value was set to $\epsilon_{0,\mathrm{ref}}=Rd_{\mathrm{ref}}\, m_e\omega_{\mathrm{ref}}^2$, where m_e denotes the free electron mass. Note that $\delta_0=\epsilon_{0,\mathrm{ref}}/(m_e\omega^2)$ is the quiver length of the driven electron. By taking $\delta_0/2=D$ we assume that the external field enforces the electrons to get from one QD to its next neighbor.

In Fig. 3 we present results demonstrating that correlation effects are important for harmonics belonging both to the first and the second plateaus of the HHG spectra. Note that (17, 19) and (53, 55) are pairs of harmonics located in the first plateau (see Fig. 1), while (143, 145) and (179, 181) are pairs of harmonics from the second plateau. As one can see, the electron correlation effects are largest for $d=1.5$ in the first case and for $d=1.3$ in the second case. For clarity, in Fig. 4 we also show the complete HHG spectrum with and neglecting electron correlations at an interdot separation $d=1.5$.

V. DISCUSSION AND CONCLUSION

The generation of high harmonics by quantum dot nanoarrays is a completely new field, and the numerical results reported here represent the first steps in this direction. We hope, of course, that our study will stimulate also experimental work in this field. Much remains to be done from the theoretical side in this area, including even a better understanding of certain features of the HHG spectra reported (but not discussed) in this paper. The generation of very high harmonics from quantum dot nanorings of the type considered here might be intriguing at a first sight: this effect seems to be counterintuitive, because photons of high-order harmonics have energies much larger than bound state energies, and the continuum is excluded from model (1) of nanoring.

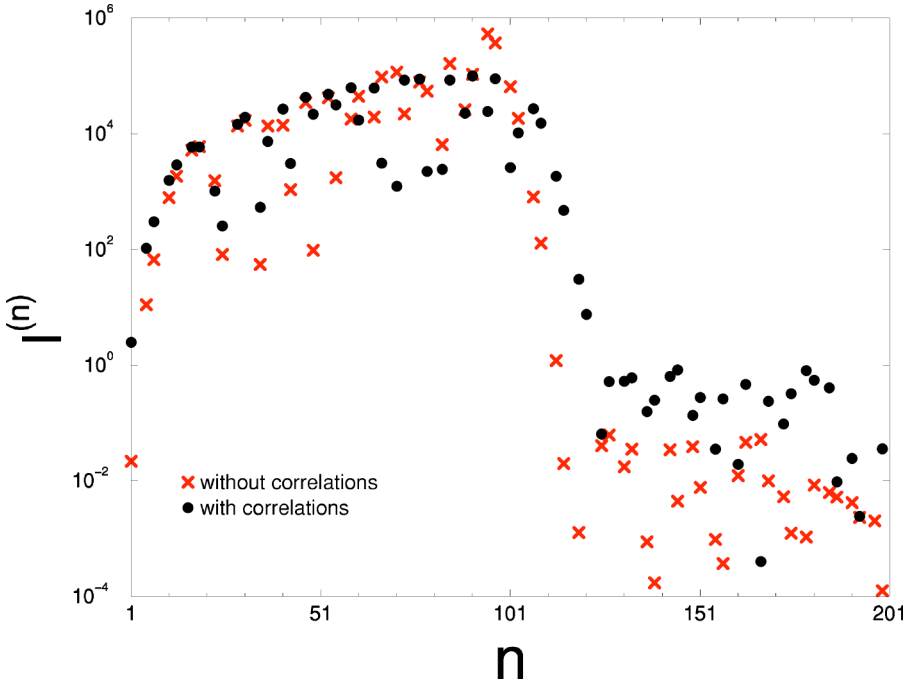

FIG. 4. The impact of electron correlations on the high harmonic generation spectra for interdot separation $d=1.5$. Full circles are results of full calculations (i.e., including electron correlations), crosses are obtained without correlations.

To qualitatively understand the HHG, we refer to the mechanism discussed in effectively bound systems, first proposed for a two-level model[34] and generalized later for N-level models with dynamical symmetry.[11] According to the findings of these references, it is not the electron excitation energy [in our case, at most $4\beta_0$ within a single-particle picture, see Eq. (1)] which is transformed into the high-order harmonic energies; rather, the energy of interaction between the nanoring and the laser field [$\sim\rho|e|E_0$, see Eqs. (2) and (3)] is converted into the energies ($n\hbar\omega$) of the emitted nth-order harmonics. Based on these considerations, a cutoff n_c

$$n_c \approx \frac{2\rho\epsilon_0}{\hbar\omega} \tag{15}$$

can be obtained for the order of the highest harmonic of the spectrum.[11] Equation (15) yields the values $n_c=17$, 35, and 53 for the parameters of of the upper, middle, and lower panels of Fig. 1, respectively.[35] Roughly, these values represent $\sim 1/3$ of those obtained by inspecting the three panels of Fig. 1. Nevertheless, this agreement is fairly good if one takes into account that the prediction of Eq. (15) is based on the treatment of *one* electrons over N sites,[11] which ignores both blocking effects due to Pauli's principle [that should be considered even within a Hartree-Fock approach of model (1) of six electrons over six sites] and correlation effects, whose importance has been emphasized (see Sec. IV). Noteworthy is especially the strong ϵ_0 dependence of n_c displayed by the panels of Fig. 1 [in very good accord to $n_c \propto \epsilon_0$ of Eq. (15)] which rules out any interpretation of the harmonic generation via transition between energy levels of the nanoring.

We believe that the message from the results reported in this work is clear. It comprises two aspects. First, from a pragmatic perspective, nanoarrays of QD's appear more promising for high harmonic generation than ordinary molecules, as evidenced by the comparison between HHG spectra of QD nanorings and the benzene molecule (see Sec. III). Unlike ordinary molecules, in view of tunability, nanoarrays of the kind we studied here, similar to those already fabricated,[14] can be designed to enhance *selectively* certain desired harmonics (see Fig. 3). Secondly, from the standpoint of basic research, it is noteworthy that electron correlations can significantly enhance the generation of high-order harmonics in both plateaus. Most encouraging from both points of view, the correlation-driven enhancement appears more pronounced in the second plateau, i.e., at higher frequencies.

Previously, HHG selection rules have been demonstrated analytically for systems consisting of a single electron (or noninteracting electrons) in an external potential with an Nth-fold rotation axis of symmetry interacting with circularly polarized laser radiation.[8,9] The present numerical results show that these selection rules are more general; they also hold for the *correlated* electron systems investigated in this work. This indication is of sufficient importance to motivate further attempts to proof selection rules analytically for more realistic cases of (strongly) correlated electron systems.

In addition, there is an interesting technical feature we have encountered in this study. To the best of our knowledge, we are not aware of a similar behavior reported previously. The part played by spatial symmetry and spin conservation in drastically reducing computational efforts in molecular physics is too well established to deserve further discussion. What we found is related to a supplementary decrease of the set of needed eigenstates due to the charge conjugation symmetry, but this issue does not simply reduce to this invariance alone. For a better understanding of the special role of the charge conjugation for the presently investigated problem, let us discuss linear response versus nonlinear response. The coefficient of linear optical absorption in the (field-free) ground state Ψ_G can be expressed by Kubo formula as (μ denotes a Cartesian coordinate x or y)[36]

$$\alpha_\mu(\omega) \propto \sum_j |\langle \Psi_G | P_\mu | \Psi_j \rangle|^2 \delta(E_j - E_G - \omega).$$

The usual, well-known, selection rules for dipole transitions apply to the set Ψ_j of eigenstates contributing to the linear optical absorption. In particular, since the ground state Ψ_G is of A_{1g} symmetry, only states Ψ_j with E_{1u} symmetry [see Eq. (5)] contribute to $\alpha_{\mu,\nu}(\omega)$. In the case of the extended Hubbard Hamiltonian employed here, an additional symmetry exists, the charge conjugation invariance (e.g., Refs. 28, and references cited therein). This further reduces the number of contributing states Ψ_j: since the ground state possesses even parity with respect to charge conjugation and the dipole operator **P** is odd (see Sec. II), only odd states contribute to $\alpha_{\mu,\nu}(\omega)$. Thus, all the eigenstates Ψ_j which contribute to the linear absorption have E_{1u}^- symmetry [see Eq. (7)]. Let us now turn to nonlinear response. As revealed by the analysis of Sec. II, a set of 175 singlet eigenstates can contribute to the HHG spectrum by accounting for spatial symmetry alone. As found for linear response, this set can be also substantially diminished by considering the charge conjugation invariance. However, the effect turns out to be more subtle in the case of nonlinear response. The set of 175 eigenstates can be further split into two disjoint blocks of (105 and 70) eigenstates [see Eqs. (7) and (8)] which do not interact via dipole among themselves. What differs from the case of linear response is the fact that each of these two blocks contains both even and odd parity eigenstates with respect to charge conjugation. It is worth emphasizing that the selection rules expressed by Eqs. (7) and (8) represent a synergetic effect of the two aforementioned symmetries, i.e., spatial symmetry and charge conjugation.

To avoid confusions let us stress that in this paper we have discussed two types of selection rules: (i) selection rules indicating that the $6\pm1, 12\pm1, \ldots$, harmonics are the only ones appearing in the nonlinear spectrum and (ii) selection rules (called synergetic here) for the symmetry of the eigenstates contributing to the HHG spectrum. Both are important, although they play different roles. The former are very important to understand the HHG spectrum. The latter cannot be employed to predict which harmonics appear (or do not appear) in the HHG spectrum, but they can be incorporated in the numerical implementation to reduce drastically the computational effort [see Eq. (12)]. While useful in all situations, such selection rules are especially desirable for easing numerical studies on nonlinear response, which are well known to be time consuming in general. This aspect becomes particularly relevant when attempting to investigate larger systems.

In conclusion, we have presented in this paper a number of results demonstrating that nanorings of Ag QD's possess interesting HHG spectra. We hope that these results, although preliminary, will encourage more theoretical and experimental studies of high harmonic generation from QD arrays.

ACKNOWLEDGMENTS

Financial support for this work provided by the Deutsche Forschungsgemeinschaft (DFG) is gratefully acknowledged. L. S. C. thanks the Fonds der Chemischen Industrie for continuous support.

*Electronic address: ioan@pci.uni-heidelberg.de; Permanent address: National Institute for Lasers, Plasmas, and Radiation Physics, ISS, RO-76900 Bucharest-Măgurele, Romania.

†Electronic address: akg_1973@yahoo.com; Permanent address: Chemistry Group, Birla Institute of Technology and Science, Pilani-333031, Rajasthan, India.

[1] P. Salières, A. L'Huillier, P. Antoine, and M. Lewenstein, Adv. At., Mol., Opt. Phys. **4**, 83 (1999); T. Brabec and F. Krausz, Rev. Mod. Phys. **72**, 745 (2000).

[2] Y. Liang, S. Augst, S. L. Chin, Y. Beaudoin, and M. Chaker, J. Phys. B **27**, 5119 (1994).

[3] H. Sakai and K. Miyazaki, Appl. Phys. B: Lasers Opt. **61**, 493 (1995).

[4] C. Lyngå, A. L'Huillier, and C.-G. Wahlström, J. Phys. B **29**, 3293 (1996).

[5] Y. Liang, A. Talebpour, C. Y. Chien, S. Augst, and S. L. Chin, J. Phys. B **30**, 1369 (1997).

[6] Y. R. Shen, *The Principles of Nonlinear Optics* (Wiley, New York, 1984).

[7] N. Ben-Tal, N. Moiseyev, and A. Beswick, J. Phys. B **26**, 3017 (1993).

[8] O. E. Alon, V. Averbukh, and N. Moiseyev, Phys. Rev. Lett. **80**, 3743 (1998).

[9] O. E. Alon, V. Averbukh, and N. Moiseyev, Phys. Rev. Lett. **85**, 5218 (2000).

[10] P. Žďánská, V. Averbukh, and N. Moiseyev, J. Chem. Phys. **118**, 8726 (2003).

[11] V. Averbukh, O. E. Alon, and N. Moiseyev, Phys. Rev. A **64**, 033411 (2001).

[12] R. Baer, D. Neuhauser, P. Žďánská, and N. Moiseyev, Phys. Rev. A **68**, 043406 (2003).

[13] M. A. Kastner, Phys. Today **46**, 24 (1996).

[14] J. R. Heath, C. M. Knobler, and D. V. Leff, J. Phys. Chem. B **101**, 189 (1997); C. P. Collier, R. J. Saykally, J. J. Shiang, S. E. Henrichs, and J. R. Heath, Science **277**, 1978 (1997); G. Markovich, C. P. Collier, and J. R. Heath, Phys. Rev. Lett. **80**, 3807 (1998); J. J. Shiang, J. R. Heath, C. P. Collier, and R. J. Saykally, J. Phys. Chem. B **102**, 3425 (1998); G. Medeiros-Ribeiro, D. A. A. Ohlberg, R. S. Williams, and J. R. Heath, Phys. Rev. B **59**, 1633 (1999).

[15] R. G. Parr, *Quantum Theory of Electronic Structure* (Benjamin, New York, 1963).

[16] F. Remacle, C. P. Collier, G. Markovich, J. R. Heath, and U. Banin, J. Phys. Chem. B **102**, 7727 (1998).

[17] F. Remacle and R. D. Levine, J. Am. Chem. Soc. **122**, 4048 (2000).

[18] F. Remacle, J. Phys. Chem. A **104**, 4739 (2000).
[19] I. Bâldea and L. S. Cederbaum, Phys. Rev. Lett. **89**, 133003 (2002).
[20] L. Salem, *The Molecular Orbital Theory of Conjugated Systems* (Benjamin, New York, 1966).
[21] Generally, estimations based on the classical spherical model [e.g., $U \approx e^2/(\varepsilon R)$] are reliable within factors ~ 1.
[22] W. B. Smythe, *Static and Dynamic Electricity* (McGraw-Hill, New York, 1968).
[23] This means l-independent values of β_0, U, V, and AO energies ϵ (mostly affected by disorder) "invisible" because they were set to zero in Eq. (1).
[24] The spatial symmetry of Hamiltonian (1) can be completely characterized by the point group C_{6v}. However, we shall use throughout the point group D_{6h} when specifying state symmetries, in order to use for QD nanorings the same notation which is usual for benzene.
[25] I. Bâldea (unpublished).
[26] R. Baer, D. Neuhauser, P. Žďánská, and N. Moiseyev, Phys. Rev. A **68**, 043406 (2003). See especially Fig. 3 of this reference.
[27] Out of the total number 924 of eigenstates, 175 eigenstates have the total spin $S=0$, 567 have $S=1$, 175 have $S=2$, and 7 have $S=3$.
[28] I. Bâldea, H. Köppel, and L. S. Cederbaum, Solid State Commun. **115**, 593 (2000); Eur. Phys. J. B **20**, 289 (2001); Phys. Rev. B **63**, 155308 (2001); **69**, 075307 (2004).
[29] N. Moiseyev, Comments At. Mol. Phys. **31**(2), 87 (1995); in *Multiparticle Quantum Scattering with Applications to Nuclear, Atomic and Molecular Physics*, edited by Donald G. Truhlar and Barry Simon, IMA Volumes in Mathematics and its Applications (Springer-Verlag, Berlin, 1996).
[30] U. Peskin and N. Moiseyev, J. Chem. Phys. **99**, 4590 (1993).
[31] When the field is turned on adiabatically, *one* Floquet state is populated, and the system is prepared in this single state. In this work we have assumed that the laser is *suddenly* turned on and, hence, *many* Floquet states are populated.
[32] C. Figueira de Morisson Faria, D. B. Milošević, and G. G. Paulus, Phys. Rev. A **61**, 063415 (2000).
[33] See, e.g., A. Fetter and J. Walecka, *Quantum Theory of Many-Particle Systems* (McGraw Hill, New York, 1971).
[34] M. Yu. Ivanov and P. B. Corkum, Phys. Rev. A **48**, 580 (1993).
[35] These n_c values are considerably larger than the value $4\beta_0/\omega = 2.88$ deduced for the parameter set of Fig. 1.
[36] To discuss the linear absorption, it makes no sense to consider circularly polarized laser radiation: according to the selection rules mentioned in Sec. I, the linear response vanishes in this case.